CI

e-med
www.e-med.org.uk

KEYNOTE LECTURE

Monday 1 October 2007, 09:00–09:30

Distinguishing benign from malignant liver tumours

Jay P. Heiken

Mallinckrodt Institute of Radiology, Washington University School of Medicine, St. Louis, Missouri, USA

Corresponding address: Jay P. Heiken, MD, Mallinckrodt Institute of Radiology, 510 South Kingshighway Blvd., St. Louis, MO 63110, USA. Email: `heikenj@wustl.edu`

Abstract

Liver masses are very common and most are benign. It is therefore important to avoid unnecessary interventions for benign lesions, while at the same time ensuring accurate diagnosis of hepatic malignancies. Many cancer patients, like the general population, have incidental benign liver lesions. In planning treatment for cancer patients, it is critical to avoid inappropriate treatment decisions based on misdiagnosis of a benign lesion as a metastasis or primary liver malignancy. This article describes the salient imaging features of the common benign liver masses and outlines a general approach to distinguishing between benign and malignant hepatic lesions.

Keywords: *Liver neoplasms; hepatic hemangioma; focal nodular hyperplasia; hepatocellular adenoma.*

Introduction

The two most common benign non-cystic liver lesions are hemangioma and focal nodular hyperplasia. Hepatocellular adenoma is considerably less common, but is important to diagnose because of its small risk of malignant transformation. A useful general approach to distinguishing benign from malignant hepatic masses is to begin by attempting to identify one or more of the imaging features diagnostic of a common benign lesion or alternatively a feature pathognomonic of a malignant hepatic lesion. These imaging features and the appropriate differential diagnostic considerations are described below. This article focuses on the use of computed tomography (CT) and magnetic resonance imaging (MRI).

Hemangioma

Hepatic hemangioma is the most common benign liver tumor, occurring in up to 7% of the normal adult population, although one prospective study identified hemangiomas in 20% of liver autopsy specimens[1]. Pathologically, hemangiomas consist of interconnected endothelial-lined vascular channels, enclosed within a loose fibroblastic stroma[2]. They are fed by hepatic artery branches, and their internal circulation is slow. They generally remain stable in size over time but may occasionally demonstrate growth[3–6].

On CT, hemangiomas are sharply defined masses that are usually hypoattenuating compared with the adjacent hepatic parenchyma on unenhanced images. However, they may be iso- or hyperattenuating in patients with hepatic steatosis. On unenhanced images the vascular components of hemangiomas have the same attenuation value as the blood within blood vessels[7,8]. Thrombosed, fibrotic, or degenerated areas that are frequently present within large hemangiomas are lower in attenuation than the vascular components. Hemangiomas have a distinctive pattern of enhancement after administration of intravenous contrast medium, characterized by sequential contrast opacification usually beginning at the periphery of the lesion as one or more nodular or globular areas of enhancement, and proceeding toward the center[7,9–13]. Fibrotic areas within the lesion do not become opacified. The feature of globular enhancement was found in one study to be 88% sensitive and 84–100% specific for differentiating hepatic hemangiomas from hypervascular metastases on single-pass, contrast-enhanced CT[14]. In another study, 94% of hepatic lesions demonstrating foci of globular enhancement were hemangiomas[13]. The time required for complete contrast 'fill-in' of a hemangioma depends upon its size. Small lesions may

become completely opacified in <1 min and appear homogeneously high attenuation on arterial or portal venous phase images, whereas large lesions may require 20 min or more for complete opacification. Small rapidly enhancing hemangiomas may be associated with adjacent hepatic parenchymal enhancement ('staining') related to arterioportal shunts[15]. The intensity of contrast opacification that occurs within the vascular spaces of a hemangioma depends on the concentration of iodine in the bloodstream. On any given image, the density of the enhanced vascular spaces approximates the density of the normal vascular structures on the same image[7,14,16]. Although some solid vascular hepatic neoplasms may show dense contrast enhancement during the early phase of the contrast bolus, the density of these lesions fades more rapidly than the density of normal vessels. Another sign that can be helpful in differentiating a malignant lesion from a hemangioma is a rim-like zone of hypoattenuation at the periphery of the mass. Such a hypoattenuating rim generally is indicative of a malignant neoplasm and is not seen with hemangiomas. Angiosarcoma is an exceedingly rare malignant liver tumor, which may have an enhancement pattern similar to that of hemangioma[17–19], but which usually can be distinguished from hemangioma on multiphase helical CT examinations[20,21]. Hemangioma typically shows areas of peripheral nodular enhancement with attenuation similar to that of the aorta during all enhancement phases and centripetal progression of enhancement. The areas of enhancement in angiosarcoma often are central in location, irregular in shape, and have a lower attenuation than that of the aorta on at least one imaging phase[20,21], although the enhancement progression may be centripetal. Thus on multiphase helical CT examinations angiosarcoma generally does not fulfill the criteria necessary to diagnose hemangioma and is more likely to simulate hypervascular metastases[20].

Magnetic resonance imaging has been shown to be useful in distinguishing hemangiomas from malignant hepatic neoplasms based on the very long T2 relaxation of hemangioma compared with other hepatic masses[22–25]. Consequently, hemangiomas appear higher in signal intensity on T2-weighted images than other hepatic neoplasms (Fig. 1A). Other features characteristic but not diagnostic of hemangioma include a sharp margin and internal homogeneity[25–29]. Hemangiomas >4 cm in diameter, however, are frequently heterogeneous in signal intensity owing to various combinations of fibrosis, hemorrhage, thrombosis, hyalinization, and cystic degeneration[30,31]. Using non–contrast-enhanced MRI and quantitative characteristics alone (i.e., T2 values or lesion-to-liver signal intensity ratios), hemangiomas can be distinguished from malignant hepatic masses with an accuracy of 81–97%[22–25,28,32,33]. When morphologic characteristics are also considered, this differentiation has been made in 90–94% of cases[25,32,34]. A helpful characteristic of hemangioma is that it demonstrates a relative increase in signal intensity on heavily T2-weighted MR images compared with moderately T2-weighted images. In contradistinction, other hepatic masses except for cysts show a relative decrease in signal intensity on more heavily T2-weighted images. However, on non-contrast-enhanced MRI, vascular metastases such as those from pheochromocytoma, carcinoid, and pancreatic islet cell tumors are occasionally indistinguishable from hemangioma because of their marked hyperintensity on T2-weighted images[35,36]. Dynamic gadolinium-enhanced MRI is helpful in making this differentiation[37–40]. Hemangiomas typically show early hyperintense peripheral nodular enhancement (Fig. 1B) with complete fill-in on delayed images. However, small lesions may show early uniform enhancement, whereas some lesions, particularly large ones, may demonstrate persistent
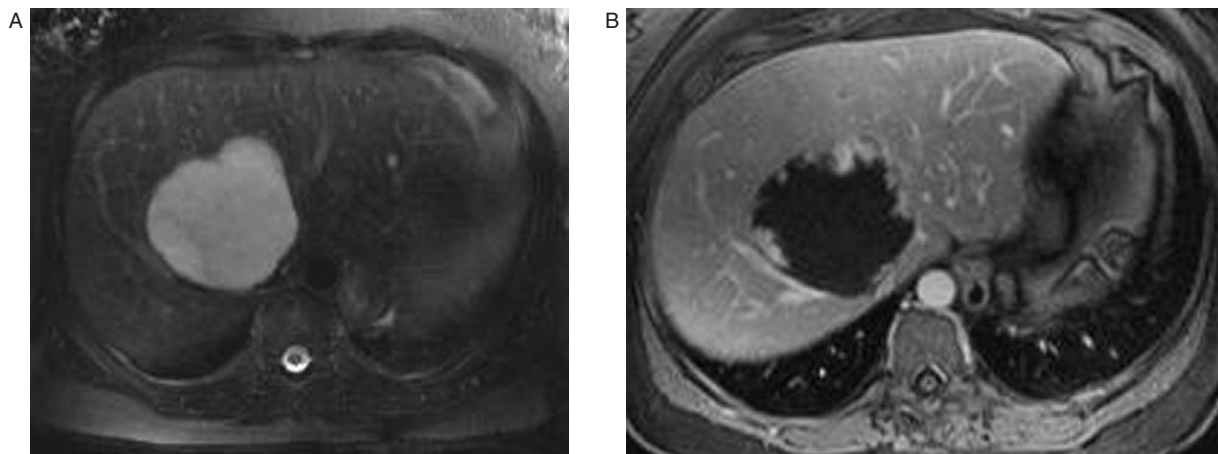
Figure 1 **Hemangioma. Unenhanced T2-weighted MR image (A) shows a large hyperintense hepatic mass. Gadolinium enhanced T1-weighted image (B) demonstrates the characteristic nodular enhancement at the periphery of the lesion. Reprinted with permission from Lee *et al*.[132].**

central hypointensity due to areas of fibrosis, thrombosis, or degeneration. Prolonged contrast material retention with signal intensity similar to the blood pool on 5–15-min delayed images is characteristic of hemangioma.

Although most small (<2 cm in diameter) hemangiomas demonstrate typical enhancement, some show an atypical pattern characterized by persistent low attenuation during both the hepatic arterial and portal venous phases of enhancement. The finding within these lesions of a small bright dot that does not progress to a focus of globular enhancement ('bright dot' sign) can be helpful in suggesting the diagnosis[41].

Uncommonly, hemangiomas may demonstrate other atypical features including hemorrhage[42], calcification[42–44], capsular retraction[42,45] and hyalinization[42,46–48]. Hyalinization of a hemangioma alters its imaging features, making diagnosis very difficult. On T2-weighted MR images a hyalinized hemangioma is only mildly hyperintense[46]. On contrast enhanced CT or MRI it typically shows no early enhancement with only slight peripheral enhancement on delayed images[46].

The approach to diagnosing hepatic hemangioma in any given patient depends upon several factors including the clinical history, the preferences of the patient and referring physician, and the imaging techniques available. In general, the following approach is recommended. Lesions discovered incidentally on ultrasound[49] or CT that are solitary and typical of hemangioma can be considered benign and ignored if the patient has no known or suspected primary malignancy. However, if the ultrasound or CT findings are atypical, or the patient has a known or suspected primary malignancy, an additional imaging test, either technetium-99m pertechnetate labeled red blood cell (RBC) scintigraphy or MRI, can provide a more definitive diagnosis. Technetium-99m pertechnetate-labeled RBC scintigraphy using single photon emission CT (SPECT) is useful if the lesion in question is ≥2 cm in diameter[34,50,51]. The demonstration on such studies of a defect on early scans with prolonged and persistent radiotracer uptake on delayed scans is virtually diagnostic of hemangioma[50,51]. For lesions <2 cm in diameter and those <2.5 cm that are located adjacent to the heart or major intrahepatic vessels, MRI is the preferred imaging test as it is more sensitive than labeled-RBC SPECT scanning for such lesions[34]. An advantage of MRI compared with labeled RBC imaging is that contrast-enhanced MRI is capable of establishing a diagnosis, even if the lesion is not a hemangioma. Only rarely is a biopsy necessary to diagnose hepatic hemangioma.

Focal nodular hyperplasia

Focal nodular hyperplasia (FNH) is the second most common benign hepatic tumor after hemangioma[52]. It occurs primarily in young women, is solitary in 75–80% of cases[53,54], and is often discovered incidentally on abdominal CT or ultrasound examinations. It typically occurs in a subcapsular location and may be pedunculated[2,52]. Although FNH is considered to be a non-encapsulated lesion, in a small percentage of cases a partial or complete fibrous capsule is present[55]. FNH is a benign vascular hepatic neoplasm composed of hepatocytes, bile ducts, blood vessels, and Kupffer cells. It frequently contains a central or eccentric fibrous scar, from which fibrous bands radiate in a spoke-wheel pattern toward the periphery. The fibrous septa, which separate the lesion into small nodules, contain thick-walled arteries and bile ductules[56]. The individual nodules are characterized by hepatocyte proliferation with lack of normal hepatic architecture, including absence of central veins or portal tracts[56]. It has been hypothesized that FNH results from a congenital vascular malformation that induces focal hepatocellular hyperplasia[57]. In contradistinction to hepatocellular adenoma, FNH is not associated with oral contraceptive use[52,58]. Although some studies suggest that oral contraceptives may promote the growth of FNH[59–64], one study has shown no effect[65].

On unenhanced CT, FNH usually appears as a homogeneous isoattenuating or slightly hypoattenuating mass. In approximately one-third of cases, a well-defined hypoattenuating scar may be identified[66–68]. Because of its prominent arterial vascular supply, FNH undergoes marked enhancement during the arterial phase of contrast-enhanced CT, becoming appreciably hyperattenuating relative to the hepatic parenchyma[66] (Fig. 2A). Except for the scar and fibrous septa when present, the enhancement of FNH is characteristically homogeneous. One or more large feeding hepatic arteries, small central and septal arteries, and early draining veins often can be identified in large lesions (Fig. 2B and C)[66, 68–70]. During the hepatic parenchymal phase, FNH usually becomes isoattenuating or nearly isoattenuating relative to normal hepatic parenchyma. Uncommonly, pseudocapsular enhancement may be seen surrounding the lesion on hepatic parenchymal phase or delayed images[55,70–72]. The pseudocapsule of FNH results from compression of surrounding liver parenchyma, perilesion vessels, and inflammatory reaction[71]. The fibrous scar, if present, usually remains hypoattenuating during the arterial phase but may show early arterial enhancement[56]. Enhancement of the scar may be seen on delayed images due to the presence of abundant myxomatous stroma[72].

On unenhanced MR images, FNH often has signal intensity characteristics similar to that of the hepatic parenchyma. On T1-weighted images it appears isointense or slightly hypointense (Figs. 3A and 4B), and on T2-weighted images isointense or slightly hyperintense relative to normal hepatic parenchyma (Figs. 3B and 4C)[55,67,73–76]. Rarely, hyperintensity within the

Figure 2   **Focal nodular hyperplasia. Contrast-enhanced, arterial phase sagittal CT image (A) shows a well-defined homogeneously enhancing hypervascular mass at the inferior edge of the right lobe of the liver. Note the non-enhancing central scar. A sagittal maximum intensity projection (MIP) image (B) demonstrates early drainage of the mass into a large hepatic vein (arrowheads). An off axis coronal MIP image (C) demonstrates that the mass has two large draining veins (arrows).**

lesion on T1-weighted images may indicate fatty change, sinusoidal dilation or copper accumulation[77–79]. The central scar, which is identified on MRI in approximately one-half to three-fourths of cases, is characteristically hypointense on T1-weighted images (Figs. 3A and 4B) and hyperintense on T2-weighted images (Figs. 3B and 4C). The hyperintensity of the scar on T2-weighted images is due to the presence of vascular channels and bile ductules[55,80]. The enhancement pattern of FNH after IV administration of a gadolinium-containing contrast agent parallels that seen on contrast-enhanced CT, including hyperintensity during the arterial phase (Figs. 3C and 4A), isointensity or near isointensity during the portal venous (hepatic parenchymal) phase (Figs. 3D and 4D), and enhancement of the scar on delayed images (Fig. 3E)[55,73,81]. Occasionally, arterial
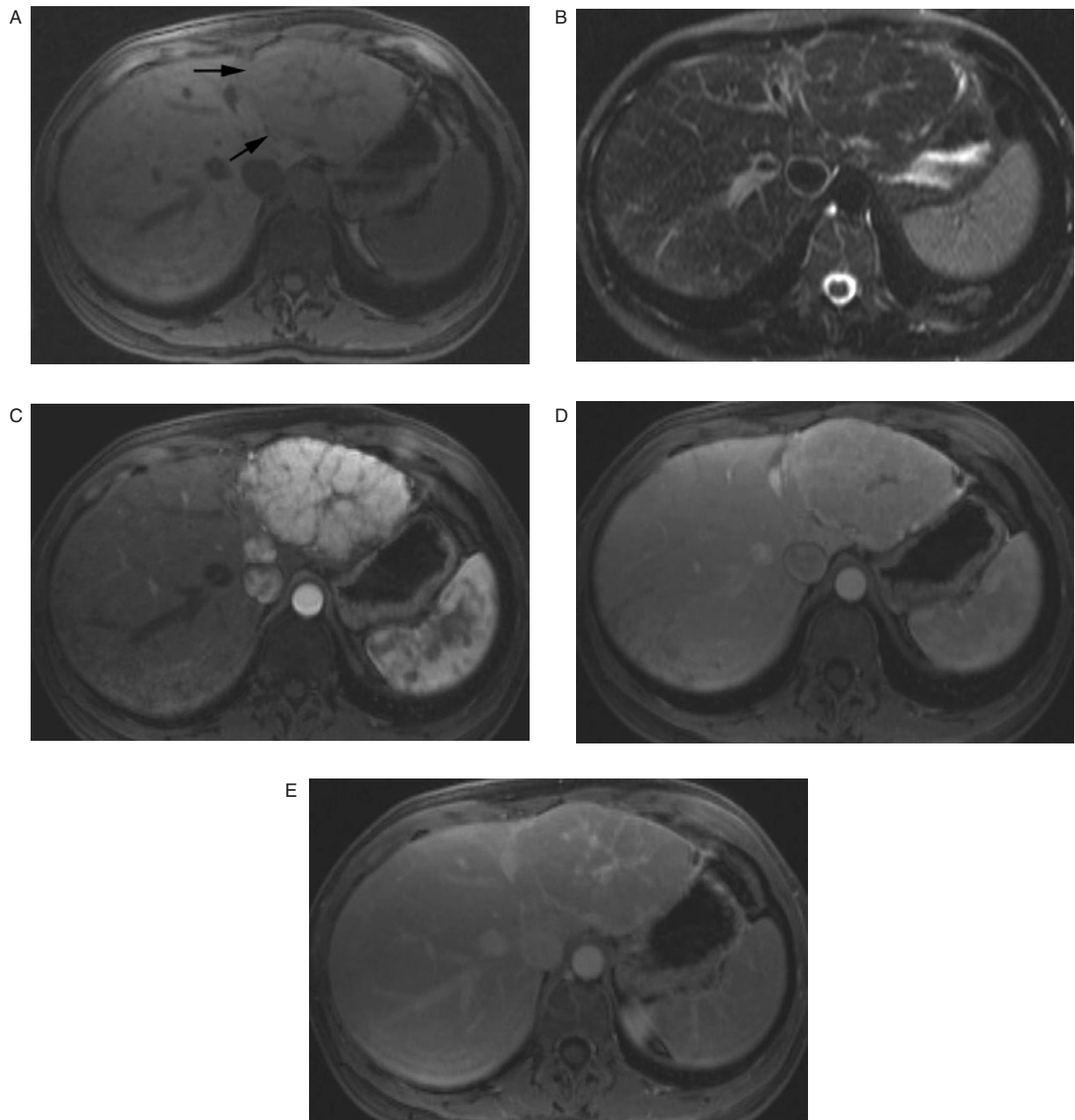
Figure 3   **Focal nodular hyperplasia. Unenhanced T1-weighted MR image (A) shows a nearly isointense hepatic mass (arrows) that contains a hypointense central scar. On a T2-weighted image (B) the mass is isointense, & the scar is hyperintense. Arterial phase gadolinium-enhanced image (C) demonstrates marked enhancement of the mass, except for the central scar and fibrous septa radiating from the scar. Portal venous phase image (D) shows rapid contrast enhancement washout of the lesion, which is now isointense with liver parenchyma. On a delayed postcontrast image (E) the mass remains isointense, but the central scar now is hyperintense.**

phase enhancement of the scar may also be seen. FNH typically shows enhancement on delayed images after administration of Mn-DPDP[82–84], Gd-BOPTA (Fig. 4E)[85,86] and Gd-EOB-DTPA[87], and shows signal loss after administration of superparamagnetic iron oxide[86,88–90]. Gd-BOPTA and Gd-EOB-DTPA are more accurate than Mn-DPDP and superparamagnetic iron oxide for diagnosing FNH because they combine dynamic arterial phase enhancement information with delayed liver-specific enhancement information[86]. In addition, diagnosis of FNH with iron oxide is based on uptake of the agent by Kuppfer cells, which may be present in relatively small numbers in some lesions. Furthermore, superparamagnetic iron oxide lacks adequate specificity to diagnose FNH because other hepatic masses including adenoma, hemangioma,
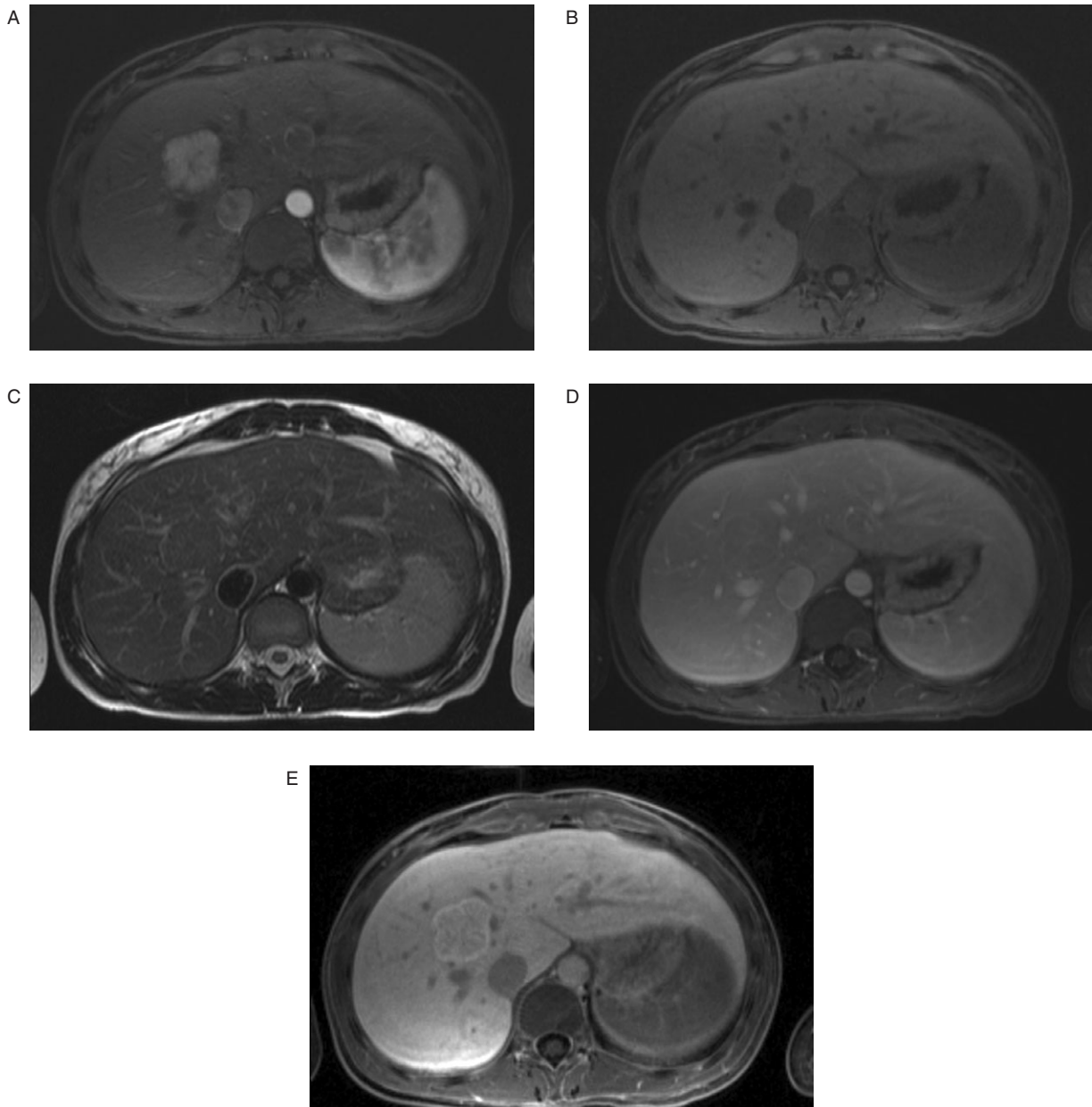
Figure 4 **Focal nodular hyperplasia. Arterial phase gadolinium-BOPTA enhanced image (A) demonstrates an intensely enhancing mass in segment 8 of the liver. Note the non-enhancing linear central scar. The mass is isointense on unenhanced T1-weighted (B) and T2-weighted (C) images. Portal venous phase image (D) shows rapid contrast enhancement washout of the lesion, which is now isointense with liver parenchyma. One hour delay image (E) demonstrates persistent enhancement of the mass, which is now hyperintense relative to the normal hepatic parenchyma.**

well-differentiated hepatocellular carcinoma, and regenerative nodular hyperplasia may also show signal loss after superparamagnetic iron oxide administration[88,91–95].

Although the typical CT and MRI features of FNH are characteristic, atypical features may be seen in 10–20% of cases[53,54]. These features may include calcification, heterogeneous enhancement, hypo- to iso-attenuation or signal intensity during the arterial phase, a low signal intensity scar on T2-weighted images, or a prominent pseudocapsule[53,70,71,96,97]. Consequently, there may be overlap between the imaging appearance of FNH and that of other hepatic masses including hepatocellular adenoma, hepatocellular carcinoma, fibrolamellar carcinoma, intrahepatic cholangiocarcinoma, hepatic hemangioma, and hypervascular metastases[67,73,81]. For example, hepatocellular carcinoma may show marked arterial enhancement and may have a central scar or an area of scar-like necrosis that is high in signal intensity on T2-weighted images[98]. However, in most cases, malignant lesions can be differentiated

from FNH because of their heterogeneous enhancement pattern. Nevertheless, in some cases it may be difficult to make a definitive diagnosis of FNH based on the CT or MRI features alone.

Hepatic scintigraphy with technetium-99m-labeled sulfur colloid may be useful in confirming the diagnosis. Because FNH contains Kupffer cells, it concentrates sulfur colloid[68,99]. In approximately one-half of cases the degree of radiotracer accumulation is similar to that of the normal hepatic parenchyma, and in 10% of cases increased concentration of colloid is seen[68,99,100]. In the remaining 40% of patients FNH appears as a photopenic defect, indicating that the Kupffer cells in the lesion have concentrated the sulfur colloid to a lesser degree than the surrounding liver. Regenerative nodules, focal hepatic steatosis, and some hepatocellular adenomas may also concentrate sulfur colloid[100,101]. However, in the proper clinical setting, the CT or MRI features in combination with normal uptake within the mass on sulfur colloid scan strongly suggest the diagnosis of FNH. The finding of increased sulfur colloid concentration is specific for FNH[100]. Another scintigraphic study that can establish the diagnosis of FNH is hepatobiliary scanning with an agent such as technetium-99m diethyl-iminodiacetic acid. The abnormal biliary drainage of FNH results in uptake and delayed excretion of the agent, revealing the lesion as a 'hot spot' within the liver on delayed images[102].

Although experience is still limited, the contrast agents that likely will be the most useful for characterizing FNH are the liver-specific hepatobiliary MR contrast agents Gd-BOPTA and Gd-EOB-DTPA. The extracellular properties of these agents can demonstrate the typical vascular enhancement pattern of FNH on dynamic post-contrast images. In addition, delayed imaging demonstrates uptake of the agent by hepatocytes within the lesion, demonstrating the hepatocellular origin of the mass[85,86]. Although other primary hepatocellular lesions such as hepatocellular adenoma and hepatocellular carcinoma also enhance with these agents, the combination of the dynamic and delayed imaging features usually is adequate to distinguish between FNH and the other lesions.

Superparamagnetic iron oxide (SPIO) MR contrast agents also are capable of characterizing FNH based on uptake of the agents by Kupffer cells within the lesion. However, because other hepatic masses including adenoma, hemangioma, well-differentiated hepatocellular carcinoma, and regenerative nodular hyperplasia also can demonstrate signal loss after SPIO administration, SPIO-enhanced MR studies performed to diagnose FNH must be interpreted with caution. One comparative study found Gd-BOPTA to be superior to SPIO-enhanced MRI for the identification and characterization of FNH[86].

A malignant neoplasm that can have an appearance very similar to FNH is fibrolamellar hepatocellular carcinoma. Both lesions tend to occur in young patients and both often contain central scars. The characteristics of the scar can be helpful in differentiating these tumors. The scar in fibrolamellar HCC is frequently calcified, whereas the scar in FNH is rarely calcified (1.4% of lesions)[96]. At MRI the scar in FNH is hyperintense on T2-weighted images and shows delayed enhancement, whereas that in fibrolamellar HCC generally is hypointense on T2-weighted images with lack of delayed enhancement. In addition, HCC does not show delayed enhancement after gadolinium-BOPTA administration (Fig. 5D).

When differentiation of FNH from other neoplasms is not possible on the basis of the imaging findings, follow-up imaging, needle biopsy, or surgical excision may be necessary. If follow-up imaging is chosen, it is important to be aware that although most lesions remain stable, a minority may demonstrate an increase or decrease in size over time[60,65,103]. If a biopsy is performed, the samples should include the fibrous scar, if present, because diagnostic bile ductules may be found only in this region of the tumor[53].

Hepatocellular adenoma

Hepatocellular adenoma is an uncommon benign primary hepatic neoplasm consisting of sheets of normal-appearing hepatocytes but lacking the normal acinar architecture of the surrounding hepatic parenchyma[2]. The hepatocytes may be rich in lipid or glycogen, and Kupffer cells are occasionally present, but bile ducts and portal tracts are absent[52,104,105]. The lesion may be surrounded by a fibrous capsule. Hepatocellular adenomas are usually solitary, but multiple adenomas are not uncommon[106,107]. They occur predominantly in women of child-bearing age, and their presence is strongly associated with the use of oral contraceptives[108,109]. Although adenomas can regress or completely disappear after withdrawal of oral contraceptives[110,111], they may continue to enlarge despite discontinuation of the drug[113]. Anabolic steroids are implicated as a cause of hepatocellular adenoma and hepatocellular carcinoma in men[52,113]. Patients with glycogen storage disease are at risk for developing multiple adenomas as well as hepatocellular carcinoma[114–118]. Hepatocellular adenoma has a tendency to undergo spontaneous hemorrhage. Although patients with an uncomplicated adenoma are usually asymptomatic, those with large or hemorrhagic lesions generally present with abdominal pain. Rare instances of malignant degeneration of hepatocellular adenomas have been reported[119–122]. Because the imaging appearance of hepatocellular adenoma is highly variable and overlaps with that of hepatocellular carcinoma, surgical resection is generally recommended.

The CT and MRI appearances of hepatocellular adenoma are varied and non-specific. On unenhanced
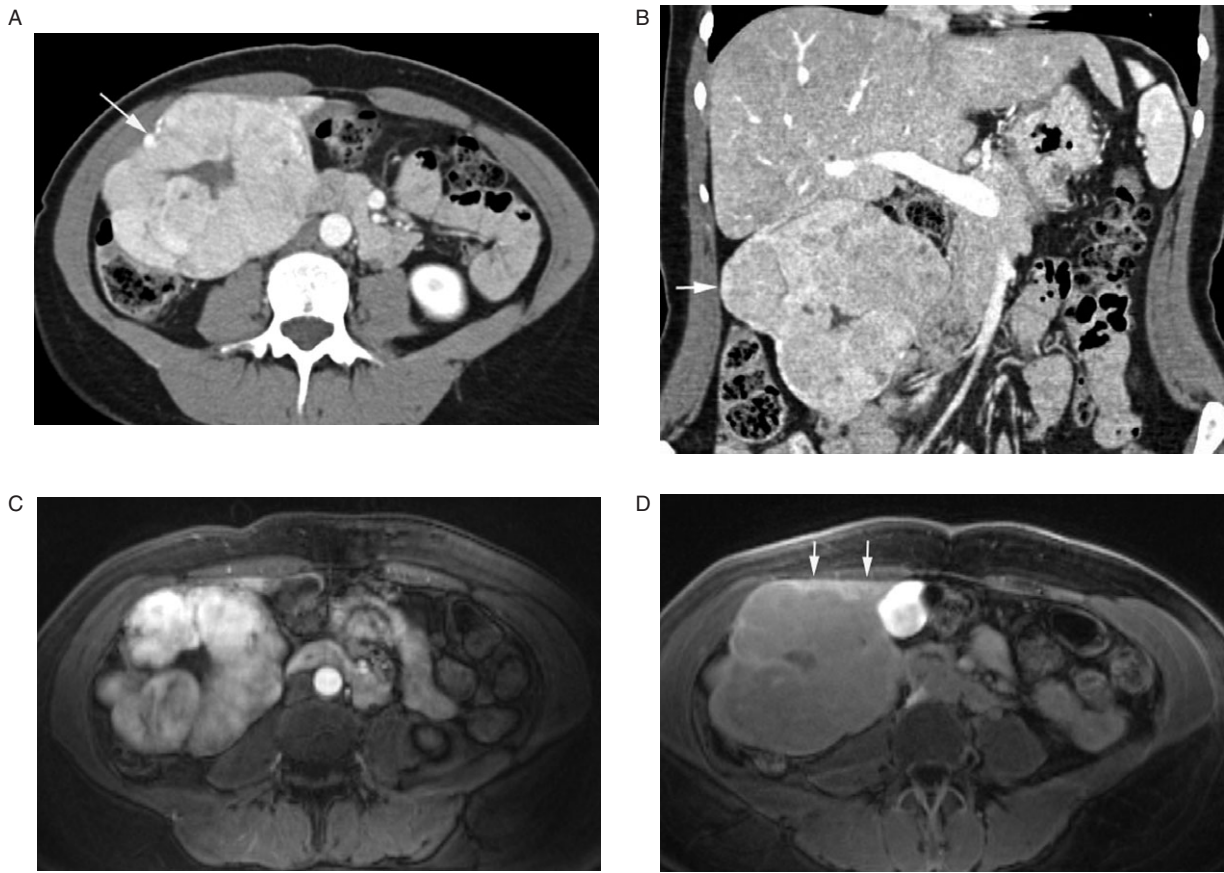
Figure 5 **Hepatocellular carcinoma. Arterial phase contrast-enhanced transaxial (A) and coronal (B) CT images shows a large exophytic hypervascular hepatic mass (arrow) that contains a large central scar. Arterial phase gadolinium-BOPTA enhanced MR image (C) shows similar findings. One hour delay image (D) after gadolinium-BOPTA administration demonstrates lack of enhancement of the mass. Note enhancement of the normal hepatic parenchyma (arrows).**

CT images the lesion may be hypoattenuating due to the presence of intracellular lipid, old hemorrhage or necrosis, or it may be hyperattenuating owing to recent hemorrhage (Fig. 6A) or large amounts of glycogen[66,106,123]. Hemorrhagic adenomas are heterogeneous, whereas uncomplicated lesions are homogeneous in appearance. Rarely, calcification may be identified[106]. After IV contrast medium administration, adenoma often demonstrates moderate enhancement during the arterial and early portal venous phases of enhancement[66]. Although there is overlap, the degree of arterial phase enhancement of most adenomas tends to be somewhat less than that seen with FNH[124]. Except for areas of necrosis, hemorrhage or fat, the enhancement is homogeneous or nearly homogeneous in 80% of cases[123]. In approximately 25% of cases, a thin tumor capsule can be identified[106]. The capsule is hypoattenuating relative to surrounding liver on hepatic arterial phase images and hyperattenuating on portal venous phase images.

The MRI appearance of adenoma is equally varied. Most lesions are heterogeneous in signal intensity[107,125,126]. The majority of hepatocellular adenomas are hyperintense to surrounding hepatic parenchyma on T1-weighted images and isointense or hyperintense on T2-weighted images[107,125]. The hyperintensity on T1-weighted images is generally related to the presence of lipid[107] or hemorrhage[125,126] in the lesion. Opposed-phase T1-weighted images may demonstrate decreased signal intensity within the lesion relative to the signal intensity on the in-phase images, indicating the presence of intracellular lipid (Fig. 7). A low-signal-intensity capsule, similar to that reported with hepatocellular carcinoma, is seen in approximately one-third of hepatocellular adenomas[75,125]. On dynamic contrast-enhanced gradient echo imaging, adenoma usually appears hyperintense to hepatic parenchyma, but may be isointense or hypointense[125]. Some hepatocellular adenomas show signal loss after administration of superparamagnetic iron oxide due to pooling of the contrast agent in peliosis-like dilated vessels or phagocytic uptake by endothelial cells[88,91].

Because of the varied appearances of hepatocellular adenoma, differential diagnosis may be difficult. When attempting to distinguish adenoma from FNH, the findings of hemorrhage or lipid within the lesion strongly
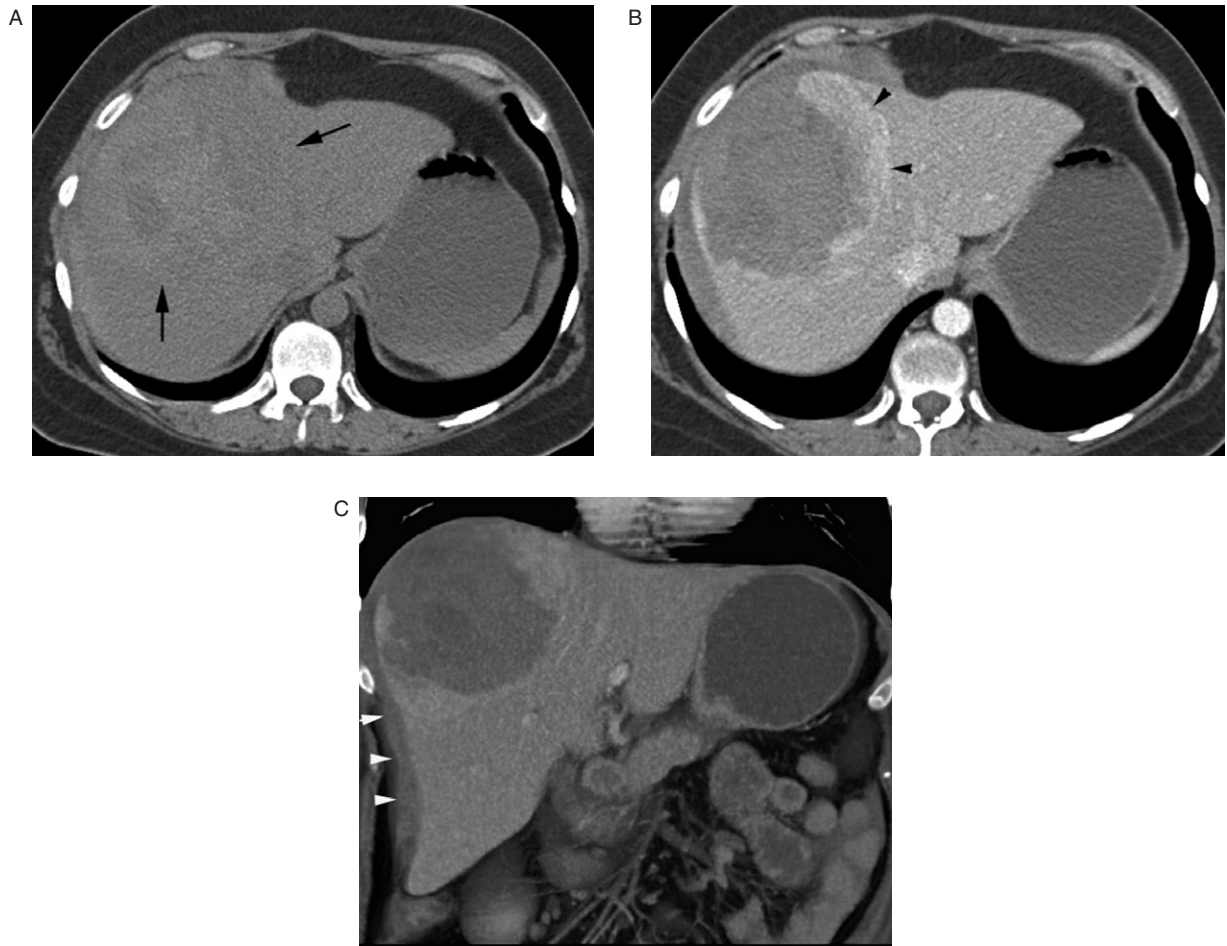
Figure 6 **Ruptured hepatocellular adenoma. Precontrast CT image (A) shows a large heterogeneous mass (arrows) near the dome of the liver. Central areas of hyperattenuation represent hemorrhage. Note the high attenuation perihepatic blood. Contrast-enhanced image (B) shows enhancement of the peripheral intact portion of the mass (black arrowheads). The hemorrhagic portion of the mass does not enhance. Note loss of integrity of the liver capsule anterolaterally. Coronal volume rendered image (C) shows the peripherally enhancing mass, ruptured liver capsule, and perihepatic blood (white arrowheads). Reprinted with permission from Lee *et al.*[132].**
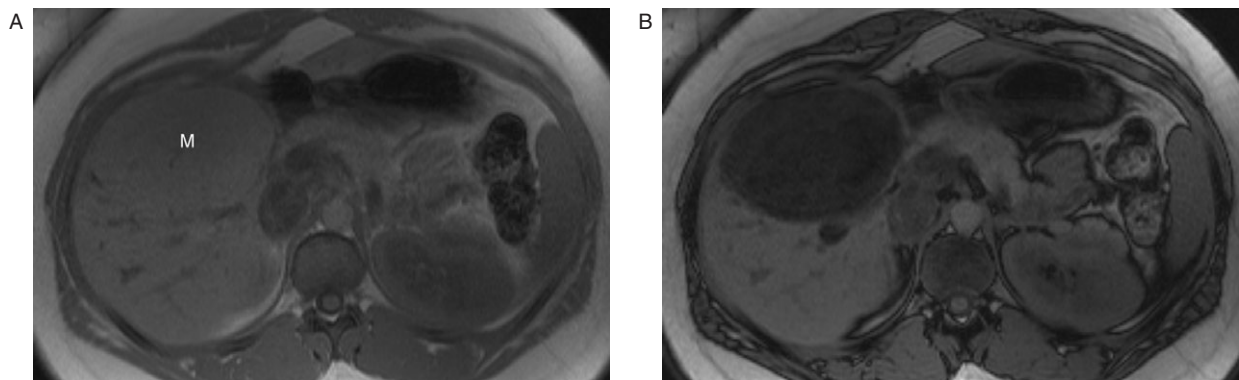
Figure 7 **Hepatocellular adenoma. In-phase T1-weighted spoiled gradient-echo MR image (A) shows a large isointense hepatic mass (M). Out-of-phase image (B) shows diffuse decrease in signal intensity within the mass due to the presence of intracellular lipid. Reprinted with permission from Lee *et al.*[132].**

support a diagnosis of adenoma. The presence of a central scar strongly supports the diagnosis of FNH, especially if the scar is hypointense on T1-weighted images, hyperintense on T2-weighted images and shows delayed enhancement. Fibrolamellar hepatocellular carcinoma usually can be distinguished from adenoma because it generally contains a large central or eccentric scar, often with calcification and radiating fibrous septa, and its enhancement is heterogeneous. In some cases, however, based on the CT or MRI appearance, it may be difficult to distinguish with confidence between hepatocellular adenoma and hepatocellular carcinoma occurring in a patient without underlying chronic liver disease.

Liver adenomatosis is a rare clinical entity, characterized by numerous hepatic adenomas (arbitrarily, more than 10) associated with increased serum alkaline phosphatase and gamma-glutamyltransferase levels, in patients without glycogen storage disease[127,128]. Both men and women are affected, although there is a female predominance (14 of 15 patients in the largest reported series)[128]. Most patients are relatively young (average age, 36 years) and have an otherwise normal liver, but many have a congenital or acquired abnormality of the hepatic vasculature, which may predispose them to the development of these adenomatous liver lesions[128]. The imaging appearance and histology of the lesions in liver adenomatosis are similar to those of sporadic hepatocellular adenomas; however, unlike most sporadic adenomas, they do not appear to be steroid dependent and do not regress with steroid withdrawal or blockage[128,129]. In fact, the size and number of lesions increases with time[128]. Patients with liver adenomatosis appear to be at increased risk for development of hepatocellular carcinoma and should be monitored with CT or MRI and serum alpha-fetoprotein levels[116,128,129].

CT and MR imaging features of malignancy

Malignant liver lesions commonly demonstrate continuous rim enhancement or diffuse heterogeneous enhancement. A hypoattenuating or hypointense halo surrounding the peripherally enhanced portion of a mass also is highly suggestive of a malignant lesion but occasionally can be seen with hepatocellular adenoma. Malignant liver lesions often have an ill-defined margin with the surrounding hepatic parenchyma, whereas benign masses tend to have a well-defined parenchymal interface. Peripheral washout on delayed images is a finding that is characteristic of malignancy and can be seen in intrahepatic cholangiocarcinoma and some hepatic metastases[130]. This finding refers to a peripheral rim that is hypointense or hypoattenuating to the center of the lesion on delayed contrast enhanced MR or CT images (Fig. 8B), and when identified enables a confident diagnosis of malignancy. Peripheral washout is seen more frequently with hypervascular as compared with hypovascular lesions[131]. Another finding pathognomonic of malignancy is portal venous or hepatic venous tumor invasion. Vascular invasion is seen most commonly with hepatocellular carcinoma, but occurs less commonly with intrahepatic cholangiocarcinoma and hepatic metastases.

Diagnostic approach

If a lesion demonstrates imaging findings diagnostic of hemangioma or focal nodular hyperplasia, no further diagnostic evaluation of that lesion is needed. If the findings are suggestive but not diagnostic of a benign lesion, then further evaluation may include interval follow-up imaging, preferably MRI, or performance of a
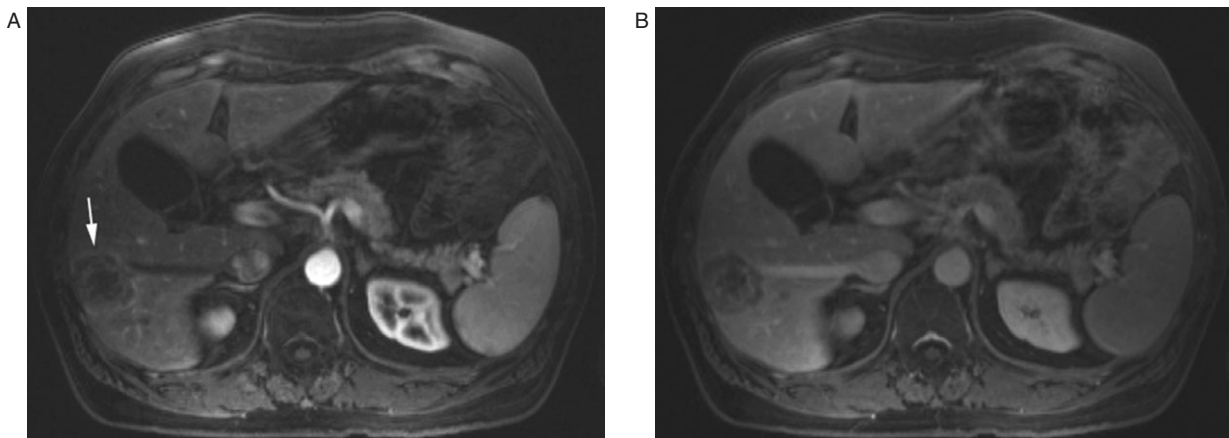
Figure 8 **Metastatic colon carcinoma. T1-weighted arterial phase gadolinium-enhanced MR image (A) shows a heterogeneously enhancing mass (arrow) in the right lobe of the liver. On an equilibrium phase image (B) the periphery of the lesion, which demonstrated enhancement during the arterial phase, is now less intense than the center of the lesion. This phenomenon is termed 'peripheral washout'.**

confirmatory imaging study (e.g., nuclear medicine or MRI with a hepatobiliary contrast agent). If these tests fail to establish the diagnosis, then continued follow-up imaging or biopsy may be necessary. If the imaging findings are diagnostic or highly suggestive of a malignant lesion, options include institution of appropriate cancer therapy or biopsy, if a histologic diagnosis is needed. In some cases, however, the imaging findings may be equivocal without findings that are highly suggestive of either a benign or malignant lesion. In such cases, management options include use of a confirmatory test, interval follow-up imaging or biopsy. Which option is most appropriate in a given situation depends upon a number of factors including how critical the diagnostic information is for immediate patient management. The patient's wishes also should be factored into the decision making process.

References

[1] Karhunen PJ. Benign hepatic tumours and tumour like conditions in men. J Clin Pathol 1986; 39: 183–8.

[2] Wright TL, Venook AP, Millward-Sadler GH. GH M-S. Hepatic tumours. In: Millward-Sadler GH, Wright R, Arthur MJP, editors. Wright's liver and biliary disease, vol 2. 3rd ed. Philadelphia: WB Saunders; 1992. p. 1079–21.

[3] Gibney RG, Hendin AP, Cooperberg PL. Sonographically detected hepatic hemangiomas: absence of change over time. AJR Am J Roentgenol 1987; 149: 953–7.

[4] Mungovan JA, Cronan JJ, Vacarro J. Hepatic cavernous hemangiomas: lack of enlargement over time. Radiology 1994; 191: 111–13.

[5] Nghiem HV, Bogost GA, Ryan JA, Lund P, Freeny PC, Rice KM. Cavernous hemangiomas of the liver: enlargement over time. AJR Am J Roentgenol 1997; 169: 137–40.

[6] Takayasu K, Makuuchi M, Takayama T. Computed tomography of a rapidly growing hepatic hemangioma. J Comput Assist Tomogr 1990; 14: 143–5.

[7] Stephens DH, Johnson CD. Benign masses of the liver. In: Silverman PM, Zeman RK, editors. CT and MRI of the liver and biliary system. Fishman EK, series editor. Contemporary issues in computed tomography, vol 12. New York: Churchill Livingstone; 1990, p. 93–127.

[8] Whitehouse RW. Computed tomography attenuation measurements for the characterization of hepatic haemangiomas. Br J Radiol 1991; 64: 1019–22.

[9] Ashida C, Fishman EK, Zerhouni EA, Herlong FH, Siegelman SS. Computed tomography of hepatic cavernous hemangioma. J Comput Assist Tomogr 1987; 11: 455–60.

[10] Freeny PC, Marks WM. Hepatic hemangioma: dynamic bolus CT. AJR Am J Roentgenol 1986; 147: 711–19.

[11] Itai Y, Furui S, Araki T, Yashiro N, Tasaka A. Computed tomography of cavernous hemangioma of the liver. Radiology 1980; 137: 149–55.

[12] Leslie DF, Johnson CD, MacCarty RL, Ward EM, Ilstrup DM, Harmsen WS. Single-pass CT of hepatic tumors: value of globular enhancement in distinguishing hemangiomas from hypervascular metastases. AJR Am J Roentgenol 1995; 165: 1403–6.

[13] Quinn SF, Benjamin GG. Hepatic cavernous hemangiomas: simple diagnostic sign with dynamic bolus CT. Radiology 1992; 182: 545–8.

[14] Leslie DF, Johnson CD, MacCarty RL, et al. Distinction between cavernous hemangiomas of the liver and hepatic metastases on CT: value of contrast enhancement patterns. AJR Am J Roentgenol 1995; 164: 625–9.

[15] Hanafusa K, Ohashi I, Himeno Y, Suzuki S, Shibuya H. Hepatic hemangioma: findings with two-phase CT. Radiology 1995; 196: 465–9.

[16] Gaa J, Saini S, Ferrucci JT. Perfusion characteristics of hepatic cavernous hemangioma using intravenous CT angiography (IVCTA). Eur J Radiol 1991; 12: 228–33.

[17] Itai Y, Teraoka T. Angiosarcoma of the liver mimicking cavernous hemangioma on dynamic CT. J Comput Assist Tomogr 1989; 13: 910–12.

[18] Mahony B, Jeffrey RB, Federle MP. Spontaneous rupture of hepatic and splenic angiosarcoma demonstrated by CT. AJR Am J Roentgenol 1982; 138: 965–6.

[19] Vasile N, Larde D, Zafrani ES, Berard H, Mathieu D. Hepatic angiosarcoma. J Comput Assist Tomogr 1983; 7: 899–901.

[20] Koyama T, Fletcher JG, Johnson CD, Kuo MS, Notohara K, Burgart LJ. Primary hepatic angiosarcoma: findings at CT and MR imaging. Radiology 2002; 222: 667–73.

[21] Peterson MS, Baron RL, Rankin SC. Hepatic angiosarcoma: findings on multiphasic contrast-enhanced helical CT do not mimic hepatic hemangioma. AJR Am J Roentgenol 2000; 175: 165–70.

[22] McFarland EG, Mayo-Smith WW, Saini S, Hahn PF, Goldberg MA, Lee MJ. Hepatic hemangiomas and malignant tumors: improved differentiation with heavily T2-weighted conventional spin-echo MR imaging. Radiology 1994; 193: 43–7.

[23] Ohtomo K, Itai Y, Furui S, Yashiro N, Yoshikawa K, Iio M. Hepatic tumors: differentiation by transverse relaxation time (T2) of magnetic resonance imaging. Radiology 1985; 155: 421–3.

[24] Ohtomo K, Itai Y, Yoshikawa K, Kokubo T, Iio M. Hepatocellular carcinoma and cavernous hemangioma: differentiation with MR imaging. Efficacy of T2 values at 0.35 and 1.5 T. Radiology 1988; 168: 621–3.

[25] Stark DD, Felder RC, Wittenberg J, et al. Magnetic resonance imaging of cavernous hemangioma of the liver: tissue-specific characterization. AJR Am J Roentgenol 1985; 145: 213–22.

[26] Choi BI, Han MC, Kim CW. Small hepatocellular carcinoma versus small cavernous hemangioma: differentiation with MR imaging at 2.0 T. Radiology 1990; 176: 103–6.

[27] Glazer GM, Aisen AM, Francis IR, Gyves JW, Lande I, Adler DD. Hepatic cavernous hemangioma: magnetic resonance imaging. Work in progress. Radiology 1985; 155: 417–20.

[28] Itai Y, Ohtomo K, Furui S, Yamauchi T, Minami M, Yashiro N. Noninvasive diagnosis of small cavernous hemangioma of the liver: advantage of MRI. AJR Am J Roentgenol 1985; 145: 1195–9.

[29] Lombardo DM, Baker ME, Spritzer CE, Blinder R, Meyers W, Herfkens RJ. Hepatic hemangiomas vs metastases: MR differentiation at 1.5 T. AJR Am J Roentgenol 1990; 155: 55–9.

[30] Choi BI, Han MC, Park JH, Kim SH, Han MH, Kim CW. Giant cavernous hemangioma of the liver: CT and MR imaging in 10 cases. AJR Am J Roentgenol 1989; 152: 1221–6.

[31] Ros PR, Lubbers PR, Olmsted WW, Morillo G. Hemangioma of the liver: heterogeneous appearance on T2-weighted images. AJR Am J Roentgenol 1987; 149: 1167–70.

[32] Mirowitz SA, Lee JK, Heiken JP. Cavernous hemangioma of the liver: assessment of MR tissue specificity with a simplified T2 index. J Comput Assist Tomogr 1990; 14: 223–8.

[33] Ohtomo K, Itai Y, Yoshida H, Kokubo T, Yoshikawa K, Iio M. MR differentiation of hepatocellular carcinoma from cavernous hemangioma: complementary roles of FLASH and T2 values. AJR Am J Roentgenol 1989; 152: 505–7.

[34] Birnbaum BA, Weinreb JC, Megibow AJ, et al. Definitive diagnosis of hepatic hemangiomas: MR imaging versus Tc-99m-labeled red blood cell SPECT. Radiology 1990; 176: 95–101.

[35] Li KC, Glazer GM, Quint LE, et al. Distinction of hepatic cavernous hemangioma from hepatic metastases with MR imaging. Radiology 1988; 169: 409–15.

[36] Rummeny E, Saini S, Wittenberg J, et al. MR imaging of liver neoplasms. AJR Am J Roentgenol 1989; 152: 493–9.

[37] Berger JF, Laissy J-P, Limot O, et al. Differentiation between multiple liver hemangiomas and liver metastases of gastrinomas: value of enhanced MRI. J Comput Assist Tomogr 1996; 20: 349–55.

[38] Mitchell DG, Saini S, Weinreb J, et al. Hepatic metastases and cavernous hemangiomas: distinction with standard- and triple-dose gadoteridol-enhanced MR imaging. Radiology 1994; 193: 49–57.

[39] Soyer P, Gueye C, Somveille E, Laissy JP, Scherrer A. MR diagnosis of hepatic metastases from neuroendocrine tumors versus hemangiomas: relative merits of dynamic gadolinium chelate-enhanced gradient-recalled echo and unenhanced spin-echo images. AJR Am J Roentgenol 1995; 165: 1407–13.

[40] Whitney WS, Herfkens RJ, Jeffrey RB, et al. Dynamic breath-hold multiplanar spoiled gradient-recalled MR imaging with gadolinium enhancement for differentiating hepatic hemangiomas from malignancies at 1.5 T. Radiology 1993; 189: 863–70.

[41] Jang HJ, Choi BI, Kim TK, et al. Atypical small hemangiomas of the liver: 'bright dot' sign at two-phase spiral CT. Radiology 1998; 208: 543–8.

[42] Vilgrain V, Boulos L, Vullierme MP, Denys A, Terris B, Menu Y. Imaging of atypical hemangiomas of the liver with pathologic correlation. Radiographics 2000; 20: 379–97.

[43] Mitsudo K, Watanabe Y, Saga T, et al. Nonenhanced hepatic cavernous hemangioma with multiple calcifications: CT and pathologic correlation. Abdom Imaging 1995; 20: 459–61.

[44] Scatarige JC, Fishman EK, Saksouk FA, Siegelman SS. Computed tomography of calcified liver masses. J Comput Assist Tomogr 1983; 7: 83–9.

[45] Brancatelli G, Federle MP, Blachar A, Grazioli L. Hemangioma in the cirrhotic liver: diagnosis and natural history. Radiology 2001; 219: 69–74.

[46] Cheng HC, Tsai SH, Chiang JH, Chang CY. Hyalinized liver hemangioma mimicking malignant tumor at MR imaging. AJR Am J Roentgenol 1995; 165: 1016–17.

[47] Takayasu K, Moriyama N, Shima Y, et al. Atypical radiographic findings in hepatic cavernous hemangioma: correlation with histologic features. AJR Am J Roentgenol 1986; 146: 1149–53.

[48] Tung GA, Vaccaro JP, Cronan JJ, Rogg JM. Cavernous hemangioma of the liver: pathologic correlation with high-field MR imaging. AJR Am J Roentgenol 1994; 162: 1113–17.

[49] Leifer DM, Middleton WD, Teefey SA, Menias CO, Leahy JR. Follow-up of patients at low risk for hepatic malignancy with a characteristic hemangioma at US. Radiology 2000; 214: 167–72.

[50] Kudo M, Ikekubo K, Yamamoto K, et al. Distinction between hemangioma of the liver and hepatocellular carcinoma: value of labeled RBC-SPECT scanning. AJR Am J Roentgenol 1989; 152: 977–83.

[51] Tumeh SS, Benson C, Nagel JS, English RJ, Holman BL. Cavernous hemangioma of the liver: detection with single-photon emission computed tomography. Radiology 1987; 164: 353–6.

[52] Craig J, Peters R, Edmonson H. Tumors of the liver and intrahepatic bile ducts (second series). Atlas of tumor pathology, vol fascicle 26. Washington, DC: Armed Forces Institute of Pathology; 1989.

[53] Carlson SK, Johnson CD, Bender CE, Welch TJ. CT of focal nodular hyperplasia of the liver. AJR Am J Roentgenol 2000; 174: 705–12.

[54] Nguyen BN, Flejou JF, Terris B, Belghiti J, Degott C. Focal nodular hyperplasia of the liver: a comprehensive pathologic study of 305 lesions and recognition of new histologic forms. Am J Surg Pathol 1999; 23: 1441–54.

[55] Vilgrain V, Flejou JF, Arrive L, et al. Focal nodular hyperplasia of the liver: MR imaging and pathologic correlation in 37 patients. Radiology 1992; 184: 699–703.

[56] Buetow PC, Pantongrag-Brown L, Buck JL, Ros PR, Goodman ZD. Focal nodular hyperplasia of the liver: radizologic-pathologic correlation. Radiographics 1996; 16: 369–88.

[57] Wanless IR, Mawdsley C, Adams R. On the pathogenesis of focal nodular hyperplasia of the liver. Hepatology 1985; 5: 1194–200.

[58] Knowles 2nd DM, Casarella WJ, Johnson PM, Wolff M. The clinical, radiologic, and pathologic characterization of benign hepatic neoplasms. Alleged association with oral contraceptives. Medicine (Baltimore) 1978; 57: 223–37.

[59] Ishak KG. Hepatic lesions caused by anabolic and contraceptive steroids. Semin Liver Dis 1981; 1: 116–28.

[60] Leconte I, Van Beers BE, Lacrosse M, et al. Focal nodular hyperplasia: natural course observed with CT and MRI. J Comput Assist Tomogr 2000; 24: 61–6.

[61] Nakayama T, Hiyama Y, Ohnishi K, et al. Arterioportal shunts on dynamic computed tomography. AJR Am J Roentgenol 1983; 140: 953–7.

[62] Nime F, Pickren JW, Vana J, Aronoff BL, Baker HW, Murphy GP. The histology of liver tumors in oral contraceptive users observed during a national survey by the American College of Surgeons Commission on Cancer. Cancer 1979; 44: 1481–9.

[63] Ross D, Pina J, Mirza M, Galvan A, Ponce L. Letter: Regression of focal nodular hyperplasia after discontinuation of oral contraceptives. Ann Intern Med 1976; 85: 203–4.

[64] Weimann A, Mossinger M, Fronhoff K, Nadalin S, Raab R. Pregnancy in women with observed focal nodular hyperplasia of the liver. Lancet 1998; 351: 1251–2.

[65] Mathieu D, Kobeiter H, Cherqui D, Rahmouni A, Dhumeaux D. Oral contraceptive intake in women with focal nodular hyperplasia of the liver. Lancet 1998; 352: 1679–80.

[66] Mathieu D, Bruneton JN, Drouillard J, Pointreau CC, Vasile N. Hepatic adenomas and focal nodular hyperplasia: dynamic CT study. Radiology 1986; 160: 53–8.

[67] Shamsi K, De Schepper A, Degryse H, Deckers F. Focal nodular hyperplasia of the liver: radiologic findings. Abdom Imaging 1993; 18: 32–8.

[68] Welch TJ, Sheedy 2nd PF, Johnson CM, et al. Focal nodular hyperplasia and hepatic adenoma: comparison of angiography, CT, US, and scintigraphy. Radiology 1985; 156: 593–5.

[69] Brancatelli G, Federle MP, Katyal S, Kapoor V. Hemodynamic characterization of focal nodular hyperplasia using three-dimensional volume-rendered multidetector CT angiography. AJR Am J Roentgenol 2002; 179: 81–5.

[70] Choi CS, Freeny PC. Triphasic helical CT of hepatic focal nodular hyperplasia: incidence of atypical findings. AJR Am J Roentgenol 1998; 170: 391–5.

[71] Hussain SM, Terkivatan T, Zondervan PE, et al. Focal nodular hyperplasia: findings at state-of-the-art MR imaging, US, CT, and pathologic analysis. Radiographics 2004; 24: 3–17(discussion 18–19).

[72] Mortele KJ, Praet M, Van Vlierberghe H, Kunnen M, Ros PR. CT and MR imaging findings in focal nodular hyperplasia of the liver: radiologic-pathologic correlation. AJR Am J Roentgenol 2000; 175: 687–92.

[73] Mahfouz AE, Hamm B, Taupitz M, Wolf KJ. Hypervascular liver lesions: differentiation of focal nodular hyperplasia from malignant tumors with dynamic gadolinium-enhanced MR imaging. Radiology 1993; 186: 133–8.

[74] Mattison GR, Glazer GM, Quint LE, Francis IR, Bree RL, Ensminger WD. MR imaging of hepatic focal nodular hyperplasia: characterization and distinction from primary malignant hepatic tumors. AJR Am J Roentgenol 1987; 148: 711–15.

[75] Rummeny E, Weissleder R, Stark DD, et al. Primary liver tumors: diagnosis by MR imaging. AJR Am J Roentgenol 1989; 152: 63–72.

[76] Schiebler ML, Kressel HY, Saul SH, Yeager BA, Axel L, Gefter WB. MR imaging of focal nodular hyperplasia of the liver. J Comput Assist Tomogr 1987; 11: 651–4.

[77] Chaoui A, Mergo PJ, Lauwers GY. Unusual appearance of focal nodular hyperplasia with fatty change. AJR Am J Roentgenol 1998; 171: 1433–4.

[78] Mathieu D, Vilgrain V, Mahfouz AE, Anglade MC, Vullierme MP, Denys A. Benign liver tumors. Magn Reson Imaging Clin N Am 1997; 5: 255–88.

[79] Prasad SR, Wang H, Rosas H, et al. Fat-containing lesions of the liver: radiologic-pathologic correlation. Radiographics 2005; 25: 321–31.

[80] Rummeny E, Weissleder R, Sironi S, et al. Central scars in primary liver tumors: MR features, specificity, and pathologic correlation. Radiology 1989; 171: 323–6.

[81] Mathieu D, Rahmouni A, Anglade MC, et al. Focal nodular hyperplasia of the liver: assessment with contrast-enhanced TurboFLASH MR imaging. Radiology 1991; 180: 25–30.

[82] Coffin CM, Diche T, Mahfouz A, et al. Benign and malignant hepatocellular tumors: evaluation of tumoral enhancement after mangafodipir trisodium injection on MR imaging. Eur Radiol 1999; 9: 444–9.

[83] Rofsky NM, Weinreb J, Bernardino ME, et al. Hepatocellular tumors: characterization with Mn-DPDP-enhanced MR imaging. Radiology 1993; 188: 52–9.

[84] Vogl TJ, Hamm B, Schnell B, et al. Mn-DPDP enhancement patterns on hepatocellular lesions on MR images. J Magn Reson Imaging 1993; 3: 51–8.

[85] Grazioli L, Morana G, Federle MP, et al. Focal nodular hyperplasia: morphologic and functional information from MR imaging with gadobenate dimeglumine. Radiology 2001; 221: 731–9.

[86] Grazioli L, Morana G, Kirchin MA, et al. MRI of focal nodular hyperplasia (FNH) with gadobenate dimeglumine (Gd-BOPTA) and SPIO (ferumoxides): an intra-individual comparison. J Magn Reson Imaging 2003; 17: 593–602.

[87] Huppertz A, Haraida S, Kraus A, et al. Enhancement of focal liver lesions at gadoxetic acid-enhanced MR imaging: correlation with histopathologic findings and spiral CT–initial observations. Radiology 2005; 234: 468–78.

[88] Grandin C, Van Beers BE, Robert A, Gigot JF, Geubel A, Pringot J. Benign hepatocellular tumors: MRI after superparamagnetic iron oxide administration. J Comput Assist Tomogr 1995; 19: 412–18.

[89] Paley MR, Mergo PJ, Torres GM, Ros PR. Characterization of focal hepatic lesions with ferumoxides-enhanced T2-weighted MR imaging. AJR Am J Roentgenol 2000; 175: 159–63.

[90] Precetti-Morel S, Bellin MF, Ghebontni L, et al. Focal nodular hyperplasia of the liver on ferumoxides-enhanced MR imaging: features on conventional spin-echo, fast spin-echo and gradient-echo pulse sequences. Eur Radiol 1999; 9: 1535–42.

[91] Denys A, Arrive L, Servois V, et al. Hepatic tumors: detection and characterization at 1-T MR imaging enhanced with AMI-25. Radiology 1994; 193: 665–9.

[92] Pauleit D, Textor J, Bachmann R, et al. Hepatocellular carcinoma: detection with gadolinium- and ferumoxides-enhanced MR imaging of the liver. Radiology 2002; 222: 73–80.

[93] Tang Y, Yamashita Y, Arakawa A, et al. Detection of hepatocellular carcinoma arising in cirrhotic livers: comparison of gadolinium- and ferumoxides-enhanced MR imaging. AJR Am J Roentgenol 1999; 172: 1547–54.

[94] Vogl TJ, Hammerstingl R, Schwarz W, et al. Superparamagnetic iron oxide-enhanced versus gadolinium-enhanced MR imaging for differential diagnosis of focal liver lesions. Radiology 1996; 198: 881–7.

[95] Yamamoto H, Yamashita Y, Yoshimatsu S, Baba Y, Takahashi M. MR enhancement of hepatoma by superparamagnetic iron oxide (SPIO) particles. J Comput Assist Tomogr 1995; 19: 665–7.

[96] Caseiro-Alves F, Zins M, Mahfouz AE, et al. Calcification in focal nodular hyperplasia: a new problem for differentiation from fibrolamellar hepatocellular carcinoma. Radiology 1996; 198: 889–92.

[97] Stanley G, Jeffrey Jr RB, Feliz B. CT findings and histopathology of intratumoral steatosis in focal nodular hyperplasia: case report and review of the literature. J Comput Assist Tomogr 2002; 26: 815–17.

[98] Hamrick-Turner JE, Shipkey FH, Cranston PE. Fibrolamellar hepatocellular carcinoma: MR appearance mimicking focal nodular hyperplasia. J Comput Assist Tomogr 1994; 18: 301–4.

[99] Rogers JV, Mack LA, Freeny PC, Johnson ML, Sones PJ. Hepatic focal nodular hyperplasia: angiography, CT, sonography, and scintigraphy. AJR Am J Roentgenol 1981; 137: 983–90.

[100] Kinnard MF, Alavi A, Rubin RA, Lichtenstein GR. Nuclear imaging of solid hepatic masses. Semin Roentgenol 1995; 30: 375–95.

[101] Lubbers PR, Ros PR, Goodman ZD, Ishak KG. Accumulation of technetium-99m sulfur colloid by hepatocellular adenoma: scintigraphic-pathologic correlation. AJR Am J Roentgenol 1987; 148: 1105–8.

[102] Boulahdour H, Cherqui D, Charlotte F, et al. The hot spot hepatobiliary scan in focal nodular hyperplasia. J Nucl Med 1993; 34: 2105–10.

[103] Kaji K, Kaneko S, Matsushita E, Kobayashi K, Matsui O, Nakanuma Y. A case of progressive multiple focal nodular hyperplasia with alteration of imaging studies. Am J Gastroenterol 1998; 93: 2568–72.

[104] Goodman ZD, Mikel UV, Lubbers PR, Ros PR, Langloss JM, Ishak KG. Kupffer cells in hepatocellular adenomas. Am J Surg Pathol 1987; 11: 191–6.

[105] Kerlin P, Davis GL, McGill DB, Weiland LH, Adson MA, Sheedy 2nd PF. Hepatic adenoma and focal nodular hyperplasia: clinical, pathologic, and radiologic features. Gastroenterology 1983; 84: 994–1002.

[106] Ichikawa T, Federle MP, Grazioli L, Nalesnik M. Hepatocellular adenoma: multiphasic CT and histopathologic findings in 25 patients. Radiology 2000; 214: 861–8.

[107] Paulson EK, McClellan JS, Washington K, Spritzer CE, Meyers WC, Baker ME. Hepatic adenoma: MR characteristics and correlation with pathologic findings. AJR Am J Roentgenol 1994; 163: 113–16.

[108] Edmondson HA, Henderson B, Benton B. Liver-cell adenomas associated with use of oral contraceptives. N Engl J Med 1976; 294: 470–2.

[109] Klatskin G. Hepatic tumors: possible relationship to use of oral contraceptives. Gastroenterology 1977; 73: 386–94.

[110] Edmondson HA, Reynolds TB, Henderson B, Benton B. Regression of liver cell adenomas associated with oral contraceptives. Ann Intern Med 1977; 86: 180–2.

[111] Kawakatsu M, Vilgrain V, Erlinger S, Nahum H. Disappearance of liver cell adenoma: CT and MR imaging. Abdom Imaging 1997; 22: 274–6.

[112] Mariani AF, Livingstone AS, Pereiras Jr RV, van Zuiden PE, Schiff ER. Progressive enlargement of an hepatic cell adenoma. Gastroenterology 1979; 77: 1319–25.

[113] Boyd PR, Mark GJ. Multiple hepatic adenomas and a hepatocellular carcinoma in a man on oral methyl testosterone for eleven years. Cancer 1977; 40: 1765–70.

[114] Coire CI, Qizilbash AH, Castelli MF. Hepatic adenomata in type Ia glycogen storage disease. Arch Pathol Lab Med 1987; 111: 166–9.

[115] Doppman JL, Cornblath M, Dwyer AJ, Adams AJ, Girton ME, Sidbury J. Computed tomography of the liver and kidneys in glycogen storage disease. J Comput Assist Tomogr 1982; 6: 67–71.

[116] Leese T, Farges O, Bismuth H. Liver cell adenomas. A 12-year surgical experience from a specialist hepato-biliary unit. Ann Surg 1988; 208: 558–64.

[117] Limmer J, Fleig WE, Leupold D, Bittner R, Ditschuneit H, Beger HG. Hepatocellular carcinoma in type I glycogen storage disease. Hepatology 1988; 8: 531–7.

[118] Miller JH, Stanley P, Gates GF. Radiology of glycogen storage diseases. AJR Am J Roentgenol 1979; 132: 379.

[119] Foster JH, Berman MM. The malignant transformation of liver cell adenomas. Arch Surg 1994; 129: 712–17.

[120] Gordon S, Reddy K, Livingstone A. Resolution of a contraceptive steroid induced hepatic adenoma with subsequent evolution into hepatocellular carcinoma. Ann Intern Med 1986; 105: 547–9.

[121] Neuberger J, Portmann B, Nunnerley HB, Laws JW, Davis M, Williams R. Oral-contraceptive-associated liver tumours: occurrence of malignancy and difficulties in diagnosis. Lancet 1980; 1: 273–6.

[122] Tao LC. Oral contraceptive-associated liver cell adenoma and hepatocellular carcinoma. Cytomorphology and mechanism of malignant transformation. Cancer 1991; 68: 341–7.

[123] Grazioli L, Federle MP, Brancatelli G, Ichikawa T, Olivetti L, Blachar A. Hepatic adenomas: imaging and pathologic findings. Radiographics 2001; 21: 877–92 (discussion 892–74).

[124] Ruppert-Kohlmayr AJ, Uggowitzer MM, Kugler C, Zebedin D, Schaffler G, Ruppert GS. Focal nodular hyperplasia and hepatocellular adenoma of the liver: differentiation with multiphasic helical CT. AJR Am J Roentgenol 2001; 176: 1493–8.

[125] Arrive L, Flejou JF, Vilgrain V, *et al.* Hepatic adenoma: MR findings in 51 pathologically proved lesions. Radiology 1994; 193: 507–12.

[126] Chung KY, Mayo-Smith WW, Saini S, Rahmouni A, Golli M, Mathieu D. Hepatocellular adenoma: MR imaging features with pathologic correlation. AJR Am J Roentgenol 1995; 165: 303–8.

[127] Flejou JF, Barge J, Menu Y, *et al.* Liver adenomatosis. An entity distinct from liver adenoma? Gastroenterology 1985; 89: 1132–8.

[128] Grazioli L, Federle MP, Ichikawa T, Balzano E, Nalesnik M, Madariaga J. Liver adenomatosis: clinical, histopathologic, and imaging findings in 15 patients. Radiology 2000; 216: 395–402.

[129] Ribeiro A, Burgart LJ, Nagorney DM, Gores GJ. Management of liver adenomatosis: results with a conservative surgical approach. Liver Transpl Surg 1998; 4: 388–98.

[130] Mahfouz AE, Hamm B, Wolf KJ. Peripheral washout: a sign of malignancy on dynamic gadolinium-enhanced MR images of focal liver lesions. Radiology 1994; 190: 49–52.

[131] Danet IM, Semelka RC, Leonardou P, *et al.* Spectrum of MRI appearances of untreated metastases of the liver. AJR Am J Roentgenol 2003; 181: 809–17.

[132] Lee JKT, Sagel SS, Stanley RJ, Heiken JP, editors. Computed body tomography with MRI correlation. 4th ed. Philadelphia: Lippincott Williams & Wilkins: 2006.